Multiscale Modeling of Spherical Symmetry Breaking in Fullerene Molecules

Laia Xiao Planas Toro

Under the direction of

Alex Atanasov
Graduate Student
Harvard University Dept. of Physics

Abstract

In this project, we study the molecular capacitances of n-carbon icosahedral fullerene molecules. Prior studies, using density functional theory (DFT), have demonstrated a remarkable linear relation between the capacitance and the fullerene radius. Although such relationships have been discovered in a number of carbon molecules, the underlying physics behind this relationship is not well-understood. Towards this end, we make use of a simple graph-based model inspired by the Hückel method to study the effect of icosahedral symmetry in causing a gap in the valence electronic structure of these molecules. By solving the associated eigenvalue problem, the orbital energies and their degeneracies are expressed in terms of two free Hückel parameters, α and β. In order to obtain these parameters, we compare the low-lying energies of the Hückel calculations to the analytically-known energies for an electron on a sphere of size equal to the fullerene radius. By adding the orbital energy gap obtained from the Hückel calculations to previous classical estimates of the capacitance, we accurately reproduce the full DFT results. This gives evidence for a simple mechanism for the capacitance of these molecules. In addition, we discuss implications for the graphene limit of infinitely large fullerenes.

Summary

In the field of nanotechnology, it is vital to understand the electronic properties of materials. In the field of energy storage, carbon materials have shown potential application. In order to study these properties, several methods are used such as density functional theory (DFT). However, these methods require substantial computational power. Therefore, in this project, we use a simple, graph-based model to calculate the electronic structure of carbon fullerenes. Carbon fullerenes are approached because of their icosahedral symmetry which simplifies the calculations and enables a comparison with spherical systems. By combining these results with earlier results using classical electrostatics we accurately reproduce the DFT results for these molecules. This gives us new insight into how these molecules store charge.

1 Introduction

In recent years, nano-scale physics has played a ubiquitous role across many exciting arenas of development in science and technology: materials science, exotic phases of matter, biochemistry, both high-performance and commercial electronics, advanced energy storage, and quantum computing. In all of these areas, an understanding of molecular systems and their respective properties is essential. At a fundamental level, all of these systems' properties are dictated by the principles of *quantum mechanics*. These systems range from atoms and molecules to superconductors [1, 2], topological materials [3], and macroscopic biological molecules [4].

In the field of nanotechnology, understanding these properties is crucial for practical studies of energy storage, charge dissipation, and the electronic structure of molecules. One of the primary modern challenges is determining the physical limitations of developing devices with exceptional energy-storage capacity (e.g. batteries and supercapacitors). Carbon materials have shown promise in this application [5], for example those based on activated graphene [6].

In studying the capacitance of molecules, the process of electron detachment and attachment plays a key role. The relevant energies are the *ionization potential I* and the *electron affinity A*. The ionization potential is the energy required to remove an electron from a molecule while the electron affinity is the energy gained from adding an electron to a neutral molecule. The energy cost of moving an electron from one molecule to another is then $I - A$. The capacitance C of the molecule, defined as the voltage difference per unit charge moved, is then given by Iafrate's formula [7]:

$$C = \frac{e^2}{I - A} = \frac{\Delta Q}{\Delta V} \tag{1}$$

where e is the charge of the electron. The capacitance is the principal quantity of study for understanding the ability of a material or molecule to store charge.

These molecular systems, which consist of many interacting electrons, are described by quantum mechanics. In particular, they fall in the regime of *quantum many-body theory*. All such quantum systems obey the Schrödinger equation, which can be written as an eigenvalue problem:

$$\hat{H}\psi = E\psi \tag{2}$$

Here $\hat{H}$ is a linear operator describing the energetics of the many-body system, called the *Hamiltonian*. ψ is a vector, called the *state vector* or sometimes *wavefunction* of the system, describing the quantum state of the electrons of the system. E is just a number: an eigenvalue of $\hat{H}$. It corresponds to the energy of the state ψ, and vectors ψ satisfying this equation are called *eigenstates* with energy E.

For systems with multiple interacting electrons, this equation becomes utterly complex. The many-body Schrödinger equation is impossible to solve analytically. For this reason, many approximate methods have been developed over the past century. The main framework for treating molecules is *molecular orbital theory* [8]. Here, the states of bonded electrons, which form the molecular orbitals, are regarded as linear combinations of the states describing individual atomic orbitals. Molecular-orbital-based methods have formed a substantial and important part of the field of computational quantum chemistry. Among these, the most thorough and computationally involved are the Hartree-Fock [9] methods, and Density Functional Theory (DFT) [10]. Despite the remarkable success, these methods require substantial computational resources and it often remains difficult to interpret the underlying mechanisms responsible for electronic structure. For instance, the most accurate calculations come from computationally intense density functional theory (DFT), despite this, this method scales poorly with increasing system size. However, simpler alternatives such as the Hartree-Fock still require substantial computational power and have the same scale limitation apart from difficulties in separating the quantum contributions from the classical ones.

Much simpler is the Hückel Method, which is a graph based method [11] that uses a

simplified Schrödinger equation to qualitatively reproduce molecular energies. Alternative, simpler approaches to Hartree-Fock and DFT often involve semiclassical physics. These use classical electrostatic approximations to model molecules as an alternative to solving the full Schrödinger equation. In such semiclassical methods, part of the system is treated classically while the remainder is left to a quantum-mechanical description [12]. In all of the above approaches, *symmetry* plays an important role. Symmetry in quantum mechanics implies that many features of molecules do not vary under certain transformations, which puts sharp constraints on the energies and states of a quantum system [13]. For this reason, taking advantage of any symmetry of the molecule greatly simplifies the calculations.

Progress in understanding aspects of many-electron systems from analytic, semi-classical, and symmetry-based points of view is likely to lead to fundamental insights in both the computational modeling of these systems, as well as in the electronic structure across a broad class of molecular systems.

Towards this goal, in this project we will study fullerenes, which are composed of connected carbon atoms that form a closed mesh. Fullerenes can look like hollow spheres, ellipsoids or tubes. These particular molecules are of widespread interest and have a very rich literature. They have many applications ranging from electrical energy storage to gene and drug delivery [14]. In this project, we will focus on fullerenes with *icosahedral symmetry*, such as the famed C_{60} molecule [15]. These molecules provide prototypical examples of fullerenes, and their symmetry structure allows them to be much more easily studied, both computationally and analytically [16]. Moreover, the molecular capacitance of this class of fullerenes exhibits remarkably smooth scaling properties that are linear in the radius of the molecules, as shown in [17]. In that paper, it was found through intensive DFT that the capacitance of such fullerenes obeys to high accuracy:

$$C = 4\pi\epsilon_0\kappa R + C_0, \quad \kappa \approx 0.562, \ C_0 \approx 1.043 \text{ au.} \tag{3}$$

This looks very similar to the *classical* capacitance scaling

$$C = 4\pi\epsilon_0 R \tag{4}$$

of conducting spheres. In the case of fullerenes, though, there is a nontrivial dielectric constant κ, as well as a nontrivial intercept C_0. Such "quasi-classical" scaling of the valence electronic properties of the molecule begs for a simple, analytic explanation.

In a more recent paper [18], it was demonstrated that the electron detachment energies of icosahedral fullerenes can be decomposed into a classical electrostatic component, by treating them as conducting spheres, but also as an inherent quantum mechanical component. This quantum aspect, related to the electron detachment energies, was conjectured to be caused by the icosahedral deviation of the molecules from being perfect spheres. Due to this, the energy levels of the molecular orbitals split [19]. In particular, it causes a split from the highest-occupied molecular orbital (HOMO) and the lowest-unoccupied molecular orbital (LUMO). This split is known as the HOMO-LUMO gap (ΔE_n) as shown in Figure 1. This energy gap is responsible for many of the electronic characteristics of materials, and is specially important in semiconductors and capacitors. Thus, understanding both the classical and quantum contributions to the capacitance of these fullerenes opens a window for developing new carbon-based materials for energy storage.
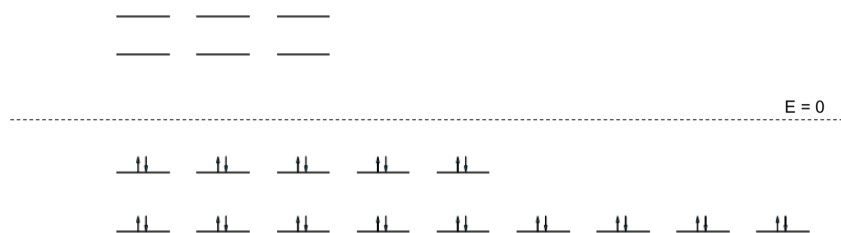

Figure 1: Highest-occupied molecular orbital (HOMO) and lowest-unoccupied molecular orbital (LUMO) in a molecular orbital diagram.

In general, the characterization of the HOMO-LUMO gap requires DFT. However, since this previous research highlights that the HOMO-LUMO gap is primarily due to the icosahedral breaking, a simpler approach can be used instead. We apply a simple, graph-based model, inspired by Hückel method, where molecules are treated as graphs in order to solve the eigenvalue problem and obtain the energies of the molecular orbitals. The fullerenes treated in this project were C_{60}, C_{180}, C_{240}, C_{540}, C_{720}, C_{960}, C_{1500} and C_{2160} which are all icosahedral fullerenes with a HOMO-LUMO gap. We choose this range of fullerenes to demonstrate the multi-scale validity of the capacitance relation, and to understand the "graphene limit" of an infinitely large fullerene.

In doing so, we observe the icosahedral symmetry from a more refined and quantitatively sound point of view. By comparing the eigenvalue spectrum with energies obtained from a spherical, free electron model, we extract the dimensionful values of the otherwise undetermined Hückel parameters and reproduced with accuracy the HOMO-LUMO gap of the system. Therefore, we are able to describe the features of these fullerene molecules, especially the larger ones. In addition, combined with previous semi-classical results for these molecules, evidence for a simple mechanism for the capacitance of these molecules is given.

2   Methods

In order to study fullerenes and observe the splitting of the energy levels caused by the icosahedral symmetry breaking from each molecule, the goal is to obtain both the HOMO and LUMO eigenvalues. From these, we can obtain the HOMO-LUMO gap. To obtain the eigenvalues, the Hückel method is used. For small enough fullerenes, like C60, the relevant molecular graphs can be constructed manually, while for larger fullerenes require a specialized program. Using a Python code, we are able to process the eigenvalues and obtain the diagram and HOMO-LUMO gap in terms of the Hückel parameters (discussed below). To obtain the

these parameters, we compare the low-lying energies of the Hückel calculations to the energies of an electron on a sphere of size equal to the fullerene radius, which are known analytically.

Hückel method

The Hückel method describes the molecular orbitals as a linear combination of atomic orbitals which determines the energies of molecular orbitals for the π-electrons. σ-orbitals are not considered due to the fact that most of the spectral and chemical properties are defined by the π-electrons. This works very well for resonant molecules with delocalized π-electrons, like the fullerenes. In this method, molecules are treated as graphs, thus every atom is a node and the edges are the bonds. We use the adjacency matrix of the graph to define the *Hückel Hamiltonian*:

$$\hat{H} = \alpha + \beta A \tag{5}$$

which plays the familiar role of $\hat{H}$ in the eigenvalue equation (2). Here α, β are the *Hückel Parameters*. Therefore, by using the Hückel method, the number of energy levels and their degeneracies are obtained in terms of two parameters α and β which correspond to the energy of a 2p electron and the interaction energy between two orbitals. It is important to emphasize that α and β are free parameters, and never evaluated in Hückel approximation. Their values must be obtained empirically. This method was chosen for its simplicity.

Python (direct construction)

We develop Python code which takes adjacency matrix for a given molecular graph and solves the associated eigenvalue problem. Once the eigenvalues are obtained, the program counts the degeneracies of the eigenvalues and finally draws the molecular orbital diagram. For C_{60} the adjacency matrix was manually constructed to be input into the code. The molecular graph is shown in Figure 2 while the spectrum is given in Figure 3.
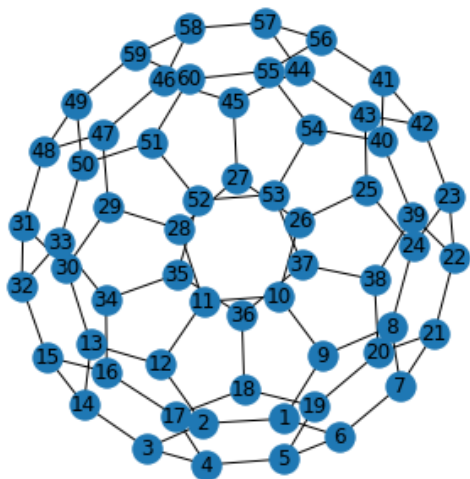
6

Figure 2: Graph of C_{60} obtained with Python.

Figure 3: Molecular orbital diagram based on the eigenvalues in units of the parameter β of C_{60}.

Fullerene (v.4.5)

With larger fullerenes, the program Fullerene (Version 4.5) [20] is used to to obtain the matrices and the eigenvalues automatically. This program enables the user to create any fullerene's adjacency matrix as well as providing a complete data set of several features such as the eigenvalues and the number of isomers of the particular molecule. To get the data of bigger fullerenes, Goldberg-Coxeter (GC) transformations are applied to smaller fullerenes. The fullerenes approached in this paper are obtained using Halma and Leapfrog transformations of C_{20}, which are special cases of GC transformations.

Comparison with Spherical model

In order to extract meaningful predictions from the Hückel method, one must know the values of α and β. For calculating the HOMO-LUMO gap it is sufficient just to know the value of β.
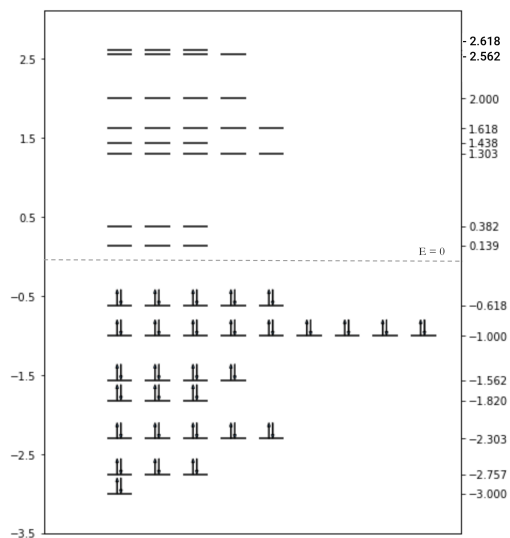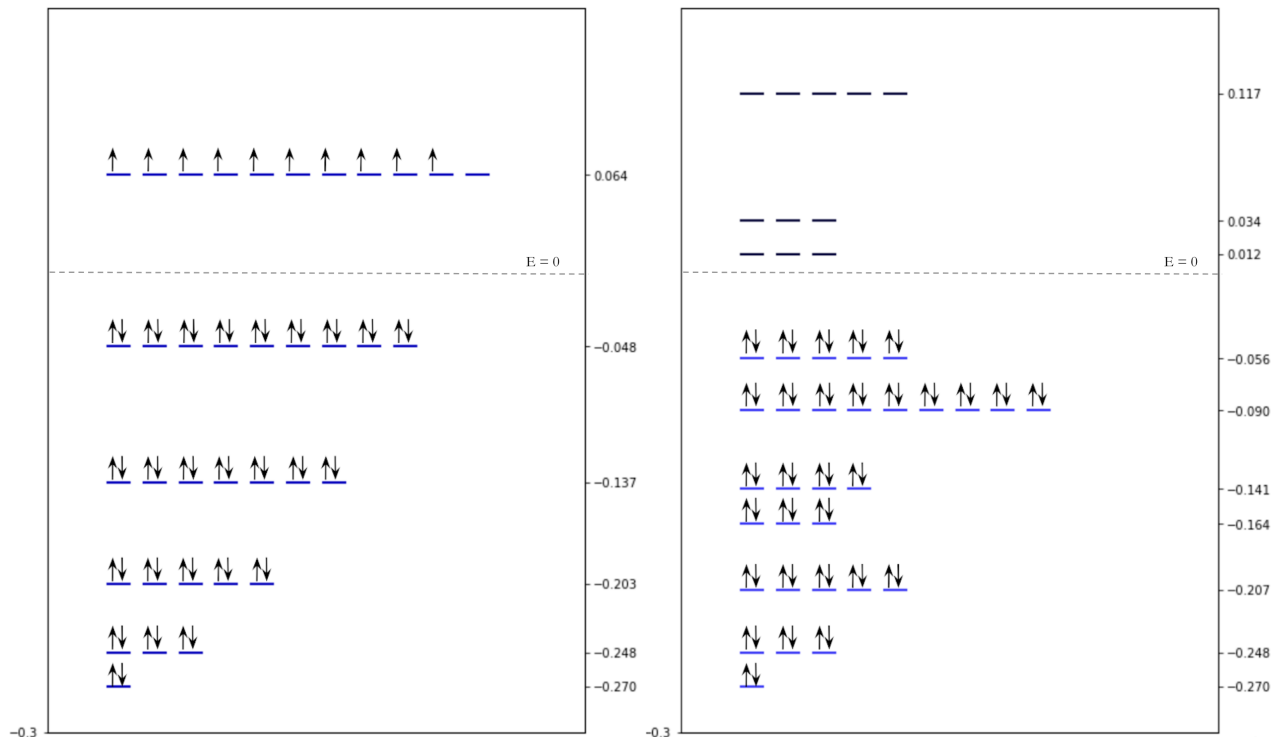
7

Figure 4: Comparison of the molecular orbital diagrams of C_{60} (right) with the energy spectrum of an electron on a perfect sphere (left). From the requirement that the low-lying energies match, an estimate for β may be extracted.

Although the analytic form of a free electron on an icosahedron is not explicitly known, the spectrum of a free particle on a *sphere* is given by the classic result

$$E = \frac{J(J+1)}{2R^2} \tag{6}$$

in atomic units. Here $J = \{0, 1, \dots\}$ is a quantum number corresponding to total angular momentum. At level J there is a $(2J + 1)$-fold degeneracy in this model. Taking R to be the fullerene's average radius, we get unambiguous predictions for the energy levels of the fullerene in the spherical approximation. In agreement with the expectation of spherical symmetry breaking, the lowest-energy states of all fullerenes considered match with the

spectrum of this spherical model. As an example, see Figure 4. By matching the three lowest-lying levels, we can extract an estimate for the value of β, and thus predict the HOMO-LUMO gap (c.f. Figure 4) .

3   Results

The energy gaps for each fullerene in units of the parameter β are calculated from the eigenvalues provided by the program Fullerene (v.4.5) as shown in Table 1. The average β estimated value is 0.097, obtained from comparing each fullerene's spectrum with the spherical system of the same average radius. It can be observed that the HOMO-LUMO gap diminishes with increasing size in fullerenes, being 0.076 atomic units (au) in C_{60} and 0.018 au C_{2160}. By adding these band gaps to previous classically predicted values of ionization potentials (I_n) [18], close approximations to the DFT values are obtained. These are depicted graphically in Figure 5.
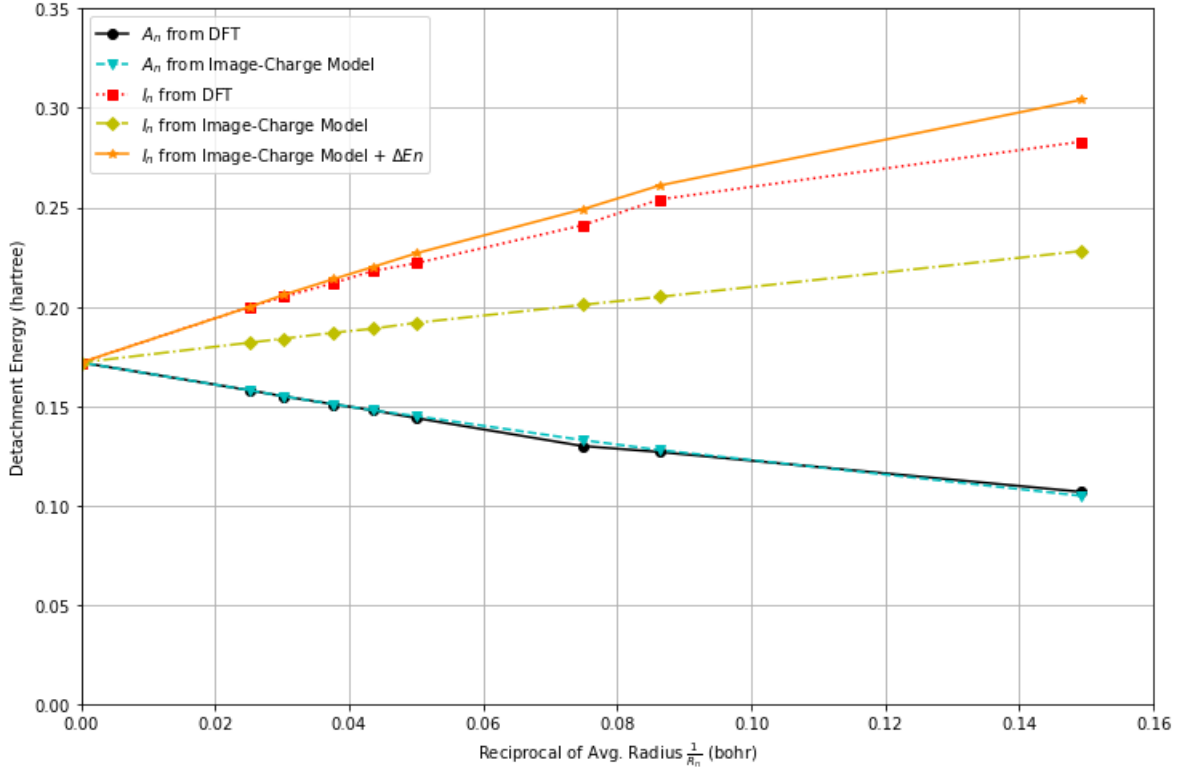
Figure 5: Icosahedral fullerene electron detachment energies (I_n and the A_n) from DFT and classical predictions depending on $1/R_n$.

The capacitance of the different fullerenes is calculated using the ionization potentials and the electron affinities as in Equation (1). These values are obtained from DFT, classical predictions and classical predictions with the energy gap. These three different capacitance relations are shown in Figure 6. We see excellent agreement between our simple calculations and the ones obtained through DFT as shown in Figure A
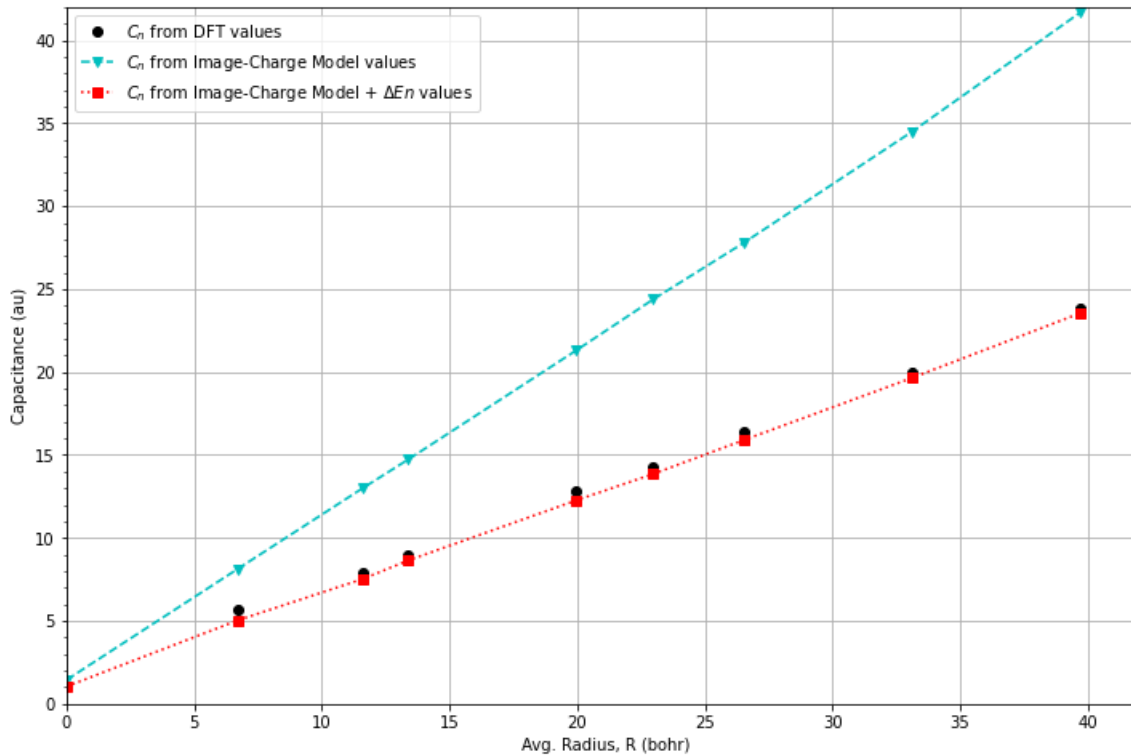
Figure 6: Capacitances depending on the fullerenes' radius obtained from DFT values, classical predicted values and classical predicted values with the band gap.

4   Discussion

The incorporation of the HOMO-LUMO gap to the values obtained classically in a prior project [18] show an accurate approximation of both the detachment electron energies and capacitance obtained from DFT, especially in larger fullerenes as shown in Figure 6 and Figure 5. These results remark the validity of what Atanasov & Ellenbogen [18] determined in a prior paper: these systems can be decomposed into a classical electrostatic component in series with an inherent quantum mechanical component (due to the symmetry breaking inducing a HOMO-LUMO gap). Figure 7 gives a circuit diagram for the total capacitance of the system, highlighting its classical and quantum component. Therefore, the expected result

was that by taking into account the quantum contributions, the results obtained would be very close to the DFT ones. On the other hand, these results also prove that despite Hückel method being a simple approach compared to DFT or other computational methods such as the Hartree-Fock method, it still provides very explicit insight into the nature of these molecules.
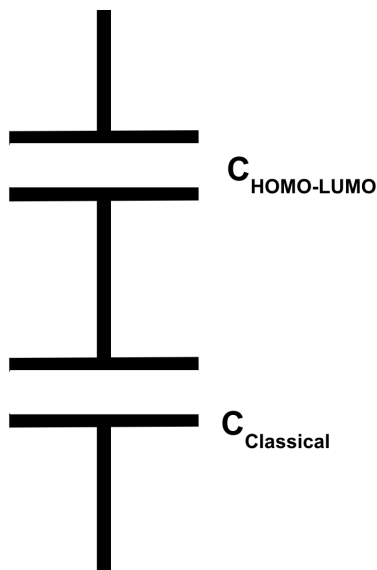

Figure 7: Total capacitance expressed by the classical capacitance together with the quantum mechanical HOMO-LUMO gap induced from symmetry breaking.

The HOMO-LUMO gap results are especially satisfying since the method we use is quite simple compared to DFT. Due to this, these calculations could have led to large estimation errors, yet we do not see this. The largest errors come from C_{60}, and our approximation only gets better for larger fullerenes. The ionization potentials, obtained by including the band gap to the classical value, only vary 0.021 au in the worst case (C_{60}) from the DFT values and exactly coincide in the best case (C_{2160}). The variation in the smaller fullerenes is because the β that determines ΔE is most dependent on the value of R in those cases. For those cases, there is an ambiguity in defining the average radius of the fullerene, since

we may want to take into account the π electron cloud in that definition. The fact that our spherical model comparison works well for large fullerenes, where ambiguity in the radius R is less relevant, leads us to conclude that this comparison is well-justified in general.

Fortunately, although C_{60} is the most uncertain value, it does not substantially affect the capacitance estimate (equation 1) since $I - A$ is largest in that case. By contrast, for large fullerenes $I - A$ becomes much smaller, leading to substantial errors in the capacitance scaling, even for relatively good estimates of I and A. The fact that we are able to so accurately reproduce the capacitance of the fullerenes for large R is quite surprising, and gives further evidence for the implications of our model.

Figure 6 shows the accuracy of these capacitance calculations. It can be observed that the values corresponding to the classical predictions with the HOMO-LUMO gap incorporation are almost the same as the DFT ones. It is important to notice that all the capacitances are linear functions despite the extraction method used which conforms with the Lewis *et al.* work [17]. The difference between them is the slope, which is more inclined in the case of classical capacitance. The other aspect of the results that stands out is the y-intercept, which is not zero as one may expect. This occurs because even for a hypothetical fullerene with radius zero, π-electrons still have a defined orbital whose radius is not null.

Apart from the capacitance and ionization potential calculations, in this project, we can see how the fullerenes' energy spectrum varies according to their size. Graphene, which can be considered as the fullerene with $R = \infty$, has a continuous spectrum with vanishing HOMO-LUMO gap. In solid-state physics this corresponds to a conductor, with no gap between the valence and conduction bands. Therefore, the band gaps are expected to decrease with increasing fullerene size. Figure 8 shows the molecular orbital diagram for C_{540}. Compared to the C_{60} or to other smaller fullerenes, its orbitals are closer to each other. A continuous-looking spectrum starts to emerge for C_{540} which will be accentuated when increasing the size of the fullerene. As shown in table 1, the HOMO-LUMO gaps decrease with larger fullerenes,
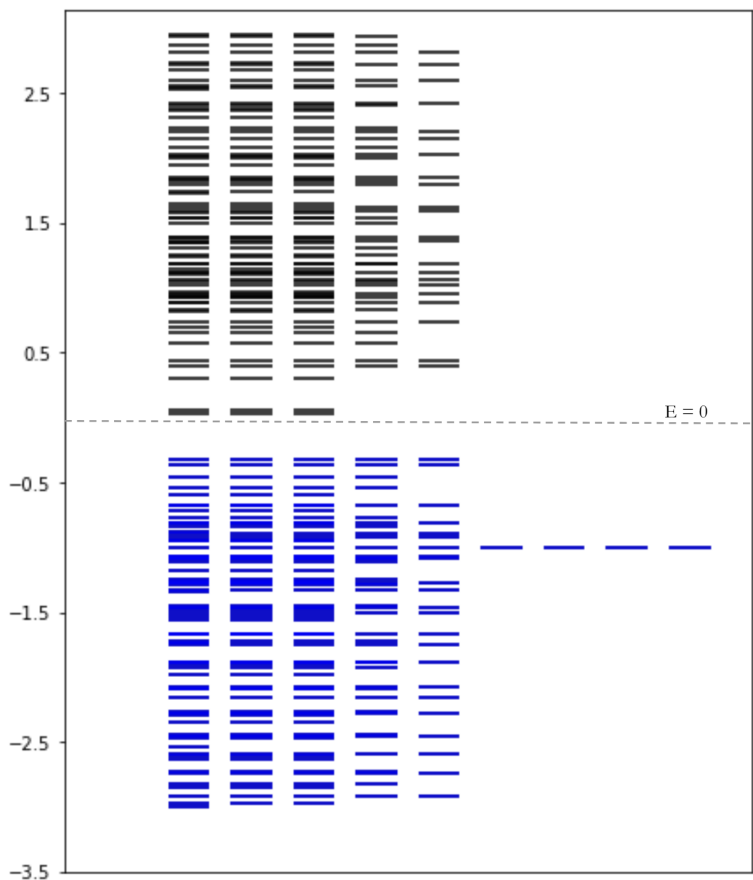
confirming this intuition.

Figure 8: Molecular orbital diagram of C_{540} with occupied orbitals in blue and empty orbitals in black.

5 Future Work

In future investigations, it would be interesting to extend this project by studying fullerenes of lower, non-icosahedral symmetry. Non-icosahedral fullerenes' HOMO-LUMO gap is smaller, thus they are expected to have an almost entirely classical capacitance [21]. "Open shell" icosahedral fullerenes, which have the formula C_{60n+20} such as C20 or C80, have a zero HOMO-LUMO gap. Therefore, we expect the capacitance to be almost entirely "classical"[16].

14

Another potential future approach would be applying this method to study carbon nanotubes, using a classical "conducting cylinder model" together with Hückel theory [22]. Finally, we hope to study poly(phenylene ethynylene) molecular wire capacitances, whose scalings appear quasi-classical as well [23].

6   Conclusion

To summarize, in this project the capacitance of different icosahedral symmetric fullerenes is approximately but accurately calculated using a simple approach based on the Hückel method combined with previous semi-classical results. This is a notable result, since the determination of these electron detachment energies usually requires substantial and intense computational power. These results strongly suggest that the capacitance can be divided into a classical component and a quantum one.

The method used especially provides accurate ionization potential data for large fullerenes. Although the ionization potential for small fullerenes has more variation from DFT results, it still provides a accurate capacitance value. Therefore, the capacitance line is reproduced with high precision.

7   Acknowledgments

References

[1] J. Bardeen, L. N. Cooper, and J. R. Schrieffer. Microscopic theory of superconductivity. *Physical Review*, 106(1):162, 1957.

[2] H. Bruus and K. Flensberg. *Many-body quantum theory in condensed matter physics: an introduction.* Oxford university press, 2004.

[3] J. E. Moore. The birth of topological insulators. *Nature*, 464(7286):194–198, 2010.

[4] J. C. Brookes. Quantum effects in biology: golden rule in enzymes, olfaction, photosynthesis and magnetodetection. *Proceedings of the Royal Society A: Mathematical, Physical and Engineering Sciences*, 473(2201):20160822, 2017.

[5] A. G. Pandolfo and A. F. Hollenkamp. Carbon properties and their role in supercapacitors. *Journal of power sources*, 157(1):11–27, 2006.

[6] Y. Zhu, S. Murali, M. D. Stoller, K. Ganesh, W. Cai, P. J. Ferreira, A. Pirkle, R. M. Wallace, K. A. Cychosz, M. Thommes, et al. Carbon-based supercapacitors produced by activation of graphene. *science*, 332(6037):1537–1541, 2011.

[7] G. Iafrate, K. Hess, J. Krieger, and M. Macucci. Capacitive nature of atomic-sized structures. *Physical Review B*, 52(15):10737, 1995.

[8] R. S. Mulliken. Lecture delivered when receiving the 1966 nobel prize in chemistry, reprinted in. *Science*, 157:13, 1967.

[9] D. Hartree. The wave mechanics of an atom with a non-coulomb central field. part i. theory and methods. *PCPS*, 24(1):89, 1928.

[10] P. Hohenberg and W. Kohn. Inhomogeneous electron gas. *Physical review*, 136(3B):B864, 1964.

[11] E. Hückel. Quantentheoretische beiträge zum benzolproblem. *Zeitschrift für Physik*, 70(3-4):204–286, 1931.

[12] V. P. Maslov and M. V. Fedoriuk. *Semi-classical approximation in quantum mechanics*, volume 7. Springer Science & Business Media, 2001.

[13] D. M. Bishop. *Group theory and chemistry.* Courier Corporation, 1993.

[14] M. S. Dresselhaus, G. Dresselhaus, and P. C. Eklund. *Science of fullerenes and carbon nanotubes: their properties and applications.* Elsevier, 1996.

[15] H. W. Kroto, J. R. Heath, S. C. O'Brien, R. F. Curl, and R. E. Smalley. C60: Buckminsterfullerene. *Nature*, 318(6042):162–163, Nov 1985.

[16] P. W. Fowler and D. Manolopoulos. *An atlas of fullerenes.* Courier Corporation, 2007.

[17] G. R. Lewis, W. E. Bunting, R. R. Zope, B. I. Dunlap, and J. C. Ellenbogen. Smooth scaling of valence electronic properties in fullerenes: From one carbon atom, to c 60, to graphene. *Physical Review A*, 87(5):052515, 2013.

[18] A. B. Atanasov and J. C. Ellenbogen. Simple, accurate electrostatics-based formulas for calculating ionization potentials, electron affinities, and capacitances of fullerenes. *Physical Review A*, 95(3):032508, 2017.

[19] F. Rioux. Quantum mechanics, group theory, and c60. *Journal of chemical education*, 71(6):464, 1994.

[20] P. Schwerdtfeger, L. Wirz, and J. Avery. Program fullerene: a software package for constructing and analyzing structures of regular fullerenes. *Journal of computational chemistry*, 34(17):1508–1526, 2013.

[21] O. V. Boltalina, E. V. Dashkova, and L. N. Sidorov. Gibbs energies of gas-phase electron transfer reactions involving the larger fullerene anions. *Chemical physics letters*, 256(3):253–260, 1996.

[22] M. Dresselhaus, G. Dresselhaus, and R. Saito. Group theoretical concepts for c60 and other fullerenes. *Materials Science and Engineering: B*, 19(1-2):122–128, 1993.

[23] J. C. Ellenbogen, C. A. Picconatto, and J. S. Burnim. Classical scaling of the quantum capacitances for molecular wires. *Physical Review A*, 75(4):042102, 2007.

A   Appendix

Num. carbon atoms	ΔE_n (Hückel)	β	ΔE_n (au)	A_n (CFT) (au)	I_n (DFT)	A_n (c.p.)	$\tilde{I}_n$ (c.p.)	$\tilde{I}_n + \Delta E_n$
60	0.757	0.100	0.076	0.107	0.283	0.105	0.228	0.304
180	0.579	0.097	0.056	0.127	0.254	0.128	0.205	0.261
240	0.496	0.097	0.048	0.130	0.241	0.133	0.201	0.249
540	0.358	0.097	0.035	0.144	0.222	0.145	0.192	0.227
720	0.321	0.097	0.031	0.148	0.218	0.148	0.189	0.220
960	0.277	0.097	0.027	0.151	0.212	0.151	0.187	0.214
1500	0.226	0.097	0.022	0.155	0.205	0.155	0.184	0.206
2160	0.190	0.097	0.018	0.158	0.200	0.158	0.182	0.200

Table 1: Ionization potentials and electron affinities of carbon fullerenes from DFT [17], classically predicted [18] and classically predicted (c.p) with the energy gap included (c.p $+\Delta E_n$) all in atomic units (au).

Num. carbon atoms	R_n (Bohrs)	Capacitance (from DFT)	Capacitance (from cp)	Capacitance (c.p $+\Delta E_n$)
60	6.705	5.68	8.13	5.03
180	11.593	7.87	12.99	7.52
240	13.366	9.01	14.71	8.63
540	19.942	12.82	21.28	12.25
720	22.990	14.29	24.39	13.86
960	26.520	16.39	27.78	15.89
1500	33.112	20.00	34.48	19.64
2160	39.711	23.81	41.67	23.55

Table 2: Capacitances of carbon fullerenes from DFT [17], classically predicted [18] and classically predicted (c.p) with the energy gap included (c.p $+\Delta E_n$) all in atomic units (au).